Short-Chain Phosphatidylinositol Conformation and Its Relevance to Phosphatidylinositol-Specific Phospholipase C†

Chun Zhou, Venkata Garigapati, and Mary F. Roberts*

Merkert Chemistry Center, 2609 Beacon Street, Chestnut Hill, Massachusetts 02167

Received July 3, 1997; Revised Manuscript Received September 30, 1997⊗

ABSTRACT: The solution conformation of chiral diheptanoylphosphatidylinositol (D- and L-inositol isomers) has been characterized by NMR spectroscopy. A positive NOE between the inositol C_2 proton and an *sn*-3 glycerol CH_2 proton has been observed in the D- but not in the L-inositol isomer of diheptanoylphosphatidylinositol (PI). Computer modeling using QUANTA constrained by this NOE and ring coupling constants suggests that the inositol ring is nearly parallel to the chain packing direction, leaving the phosphate ester accessible to attack by phosphatidylinositol-specific phospholipase C enzymes. In this model, the hydroxyl groups in the 2- and 6-positions of inositol form hydrogen bonds with the *pro-R* and ester oxygens, respectively. Chemical shifts and ^{13}C spin−lattice relaxation times were also used to assess conformation and lipid dynamics in monomer and micelle states. The ^{13}C T_1's of inositol C_2 and C_6 in monomeric phosphatidylinositol were markedly less than for other inositol ring carbons. These results are consistent with the hydrogen bonds to the phosphate constraining the motions of C_2 and C_6. Diheptanoylphosphatidyl-2-*O*-methylinositol is a good inhibitor of PI-specific phospholipase C because it blocks the initial phosphotransferase step in PI hydrolysis. Introduction of the methyl group on the C-2 hydroxyl group lowers the CMC of the derivative compared to diheptanoylphosphatidylinositol. However, an NOE between an *sn*-3 glycerol proton and the inositol C_2 proton constrains the orientation of the inositol ring with respect to the glycerol backbone in a conformation similar to diheptanoylphosphatidylinositol. Modeling of the 2-*O*-methylinositol derivative suggests that the methyl group blocks one side of the phosphate, consistent with the observation that nonspecific phospholipase C enzymes which are able to hydrolyze PI, albeit poorly, are unable to hydrolyze diheptanoylphosphatidyl-2-*O*-methylinositol.

Diacylphosphatidylinositol (PI)[1] and its phosphorylated derivatives exhibit key roles in the transduction of extracellular signals into cells (*1*, *2*). PI-specific phospholipase C (PI-PLC) enzymes hydrolyze PI derivatives to generate two intracellular second messengers, diacylglycerol and inositol phosphates (*3*, *4*). PI is also a precursor of protein anchors (*5*). Bacterial PI-PLC enzymes cleave these glycosylphosphoinositol anchors to release a number of membrane-bound proteins (*6*−*8*). For both these types of activities, an analysis of PI conformation and dynamic behavior is important to understanding its interaction with the enzymes. The X-ray crystal structures of several lipids provide an important data base for examining lipid structure (*9*, *10*). In crystal structures as well as in solution, the conformations of phosphatidylcholine and phosphatidylethanolamine have the lipid headgroup oriented roughly parallel to the membrane surface with the glycerol backbone parallel to the axis of the fatty acyl chains (*10*−*12*). In contrast, the headgroups of many glycolipids are more or less perpendicular to the membrane surface and point out into the aqueous phase (*13*−*15*). Little information is available for PI structures. Previous work has used PI isolated from natural sources, therefore, heterogeneous in chain length and unsaturation, or synthetic long-chain PI solubilized in organic solvent (DMSO or methanol) or dispersed in water to form a lamellar phase analyzed by ^1H NMR and ^2H NMR (*16*−*18*). While a ^2H NMR study provided possible structures, there were not enough constraints to orient the inositol ring with respect to the glycerol backbone or acyl chains. Computational modeling identified six possible 'tilted' orientations all of which were consistent with the ^2H NMR data.

In order to use the full power of high-resolution NMR for structural analyses, a monomeric or micellar PI is extremely useful. We have previously synthesized the D- and L-inositol isomers of short-chain PI (*19*) and PI analogs with a methoxy group on the inositol C-2 (*20*). ^{31}P NMR was used to monitor PI-PLC (*Bacillus thuringiensis*) activity toward these molecules (*21*). The results showed that the D-inositol PI isomer was an absolute stereochemical requirement for PI-PLC; the L-inositol isomer was neither a substrate nor an inhibitor. Furthermore, 2-methoxy-PI was a good inhibitor of PI-PLC enzymes. The present work presents a detailed NMR analysis of the conformation of these short-chain PI molecules in both monomer and micellar states. Coupling constant analysis and NOE data address the difference between D- and L-inositol isomers as well as the similarity of 2-methoxy-PI to diC_7PI. QUANTA computational modeling provides a likely orientation of the inositol ring with

† This work has been supported by NIH Grant GM 26762 (to M.F.R.).

* To whom correspondence should be addressed. Email: mary.roberts@bc.edu. FAX: (617)-552-2705. Phone: (617)-552-3616.

⊗ Abstract published in *Advance ACS Abstracts,* December 1, 1997.

[1] Abbreviations: PI-PLC, phosphatidylinositol-specific phospholipase C; PI, phosphatidylinositol; diC_nPI, diacylphosphatidylinositol; NOE, nuclear Overhauser effect; CMC, critical micelle concentration; T_1, spin−lattice relaxation time; COSY, ^1H correlation spectroscopy; NOESY, nuclear Overhauser effect spectroscopy; HMQC, heteronuclear multiple quantum coherence.

S0006-2960(97)01617-6 CCC: $14.00

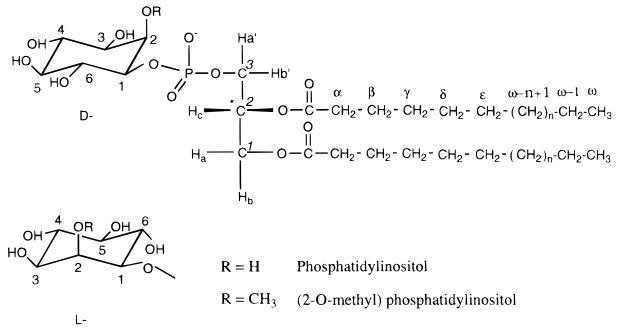

FIGURE 1: Structure and numbering scheme for phosphatidylinositol and its 2-methoxyinositol derivative structure.

respect to the interface. ^{13}C relaxation times characterize the internal motion of the PI molecule and highlight differences between monomers and aggregated PI. These results are discussed in light of PI-PLC and nonspecific PLC activities.

MATERIALS AND METHODS

Synthesis of Short-Chain PI and Derivatives. DiC_7PI isomers with D-inositol and L-inositol stereochemistry and racemic diC_6PI were synthesized and purified as described previously (*19*). The PI analog with a methoxy group on the inositol C-2, $diC_7P(2\text{-}OCH_3)I$, was also synthesized and purified as described previously (*20*). The structures of PI and PI analog are shown in Figure 1.

Enzyme Assays. PI-PLC and nonspecific PLC activities toward short-chain PI and analogs were measured by ^{31}P NMR spectroscopy as described previously (*22*, *23*). PLC enzymes from *Listeria monocytogenes* were provided by Dr. Howard Goldfine, University of Pennsylvania.

^1H NMR Analysis. 500 MHz ^1H NMR spectra were obtained with a Varian Unity 500 spectrometer using an indirect probe. ^1H T_1 values were measured using the inversion recovery method. All 2D spectra were acquired in a phase-sensitive mode using hypercomplex data sets. The ^1H carrier was set on the residual HDO resonance, and transmitter presaturation pulse sequences were used. There were 2048 points in the F2 and 256 points in F1 dimension. Zero filling was employed, and final spectra contained 2K $\times$ 2K real points. A Gaussian weighting function was most commonly used in both dimensions. Short-chain PI or PI analog samples were dissolved in D_2O. The sample for NOESY was degassed by freeze−thaw cycles. NOESY spectra were recorded with 0.5−1.0 s mixing times. A BIRD null pulse was used in the HMQC sequence with a 0.35 s null time. Volume integration of NOE cross-peaks was used to estimate distances by assuming that NOE $\propto 1/r^6$. The inositol ring is fairly rigid, and the distances between axial and equatorial or between axial and axial protons can be used as an internal reference. We have used the intensity of equatorial H_2 and axial H_1 or H_3 cross-peaks (with a distance of 2.4 Å) as the appropriate reference. The NMRi program (New Methods Research, Inc.) was used for the peak analysis and curve fitting to obtain the volume of cross-peaks.

^{13}C T_1 Measurements. ^{13}C relaxation rates can provide direct information concerning the dynamic behavior at specific sites in a molecule. The sensitivity of the measurement can be increased significantly by using the more sensitive proton resonance to monitor changes in ^{13}C magnetization. Overlapping ^{13}C resonances can also be separated by ^1H chemical shifts. There are several pulse sequences reported for selectively measuring T_1 for methine or methyl carbon that combine DEPT or INEPT methods. These pulse sequences are very useful for studying backbone (*24*) or side chain (*25*) dynamics in proteins. The pulse sequences for T_1 measurement of methine were edited using the C language and compiled for the 500 MHz Varian NMR instrument. There were 2048 points in F_2, and 64 scans were acquired per t_1 increment. Considering that the relaxation time of ^1H attached to ^{13}C is much shorter than attached to ^{12}C, a 3 s relaxation delay was used between each scan. Seven spectra were recorded with τ delays of 0.01, 0.05, 0.10, 0.20, 0.50, 1.00, and 3.00 s. The relaxation rate was calculated from peak heights of the heteronuclear resonances. Three-parameter nonlinear fitting of intensity at a given τ, $I(\tau) = I_\infty - (I_\infty - I_o)\exp(-R_1\tau)$, was used with $T_1 = 1/R_1$.

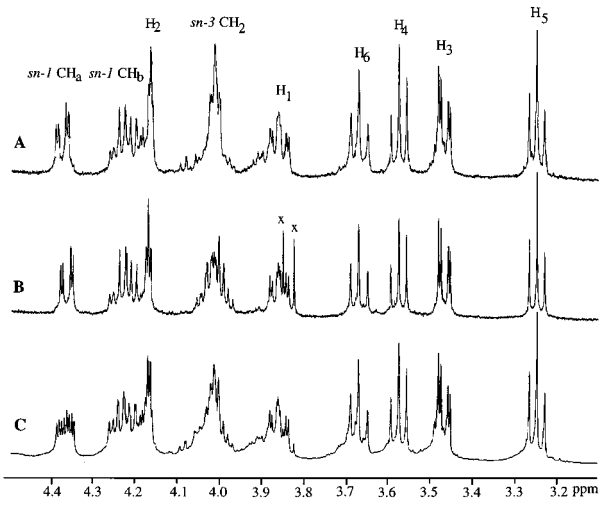

FIGURE 2: 500 MHz ^1H spectra of inositol and the backbone region of monomeric phosphatidylinositol: (A) 2.7 mM diC_7P(D-)I; (B) 2.5 mM diC_7P(L-)I; and (C) 11 mM diC_6P(D+L)I. The resonance labeled 'x' is an impurity.

RESULTS

Backbone Conformation of Phosphatidyl D- and L-Inositol Isomers. ^1H NMR spectra of monomeric diC_6PI and micellar diC_7PI were nearly identical, indicating only small conformational changes occurred upon aggregation of the lipid. Both lipids gave rise to high-resolution NMR spectra with lines sufficiently narrow to resolve spin−spin interactions. ^1H spectra of PI were easily assigned by a simple COSY experiment. Spectra of the inositol and backbone region are shown in Figure 2. The inositol ^1H chemical shifts occurred in the order H_5, H_3, H_4, H_6, H_1, and H_2 from high to low field. The chemical shifts of H_a (low-field proton in *sn*-1 backbone) and H_2 (proton at the 2-position of inositol) were quite different for the D- and L-inositol isomers. In the D-inositol isomer, H_a was shifted downfield by 6 Hz and H_2 shifted upfield by 2 Hz. $^1H-^1H$ coupling constants were the same in D- and L-inositol isomers except for the *sn*-3 methylene (Table 1). The *sn*-3 proton chemical shifts were also different such that, in the D-inositol isomer, H_a' and H_b' were magnetically more similar than in the L-isomer (Figure 3). These differences in magnetic environment indicated a significant conformational difference between the two PI species. The *sn*-1 CH_2 glycerol protons gave rise to an eight line spectrum characteristic of an ABM system. An analysis of glycerol backbone *sn*-1 CH_2 and *sn*-2 CH coupling

Table 1: Coupling Constants of Short-Chain Phosphatidylinositols (Hz)

coupling constant[a]	diC$_7$P(D-)I	diC$_7$P(L-)I
J_{1-2}	2.5	2.7
J_{2-3}	2.7	2.8
J_{3-4}	10.0	10.0
J_{4-5}	9.4	9.3
J_{5-6}	9.3	9.5
J_{6-1}	10.0	10.0
J_{1-P}	8.4	8.4
J_{a-b}	12.3	12.3
J_{a-c}	2.8	2.9
J_{b-c}	7.0	7.0
$J_{a'-c}$	6.6	4.2
$J_{b'-c}$	3.3	5.9
$J_{a'-b'}$	11.3	11.3
$J_{a'-P}$	2.6	5.8
$J_{b'-P}$	2.6	0.7

[a] H_a is the downfield proton of the backbone *sn*-1 CH_2, while H_b is the highfield proton in *sn*-1 CH_2, H_c is the *sn*-2 CH proton, $H_{a'}$ is the downfield proton, and $H_{b'}$ is the highfield proton of the backbone *sn*-3 CH_2 multiplet.

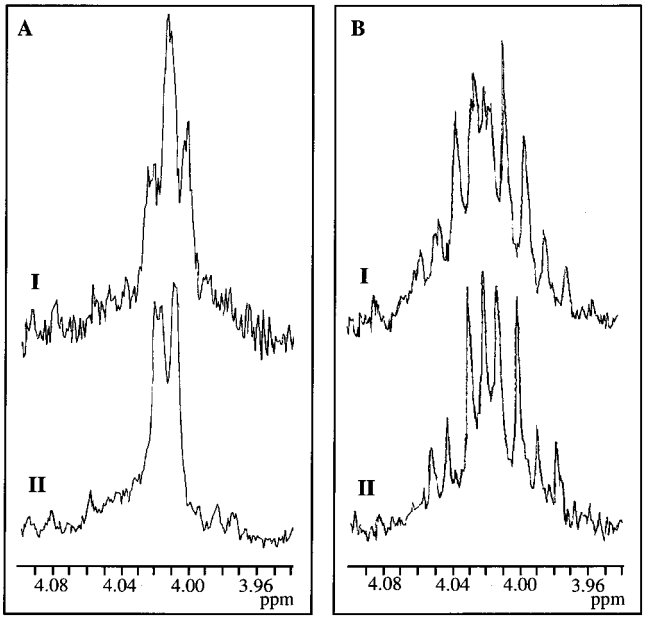

FIGURE 3: ^{1}H spectra of the *sn*-3 CH_2 region of (A) diC$_7$P(D-)I and (B) diC$_7$P(L-)I. I exhibits the ^{31}P coupled spectra, and II presents the ^{31}P decoupled spectra.

constants (J_{ab}, J_{ac}, J_{bc}) indicated that the preferred conformation of the PI glycerol backbone was the same as for other phospholipids with the two rotamers preferred where the fatty acyl chains were packed together (*26*, *27*). The protons of the *sn*-3 CH_2-OP group were also nonequivalent but to a lesser extent. This group was analyzed as an ABMX system (X = ^{31}P). The estimated coupling constants are summarized in Table 1.

^{1}H−^{31}P long-range coupling can provide information on a critical dihedral angle. The J_{H-P} coupling constant is the same for inositol C(1)H in both D- and L-inositol isomers. However, the interactions of the glycerol backbone *sn*-3 protons with ^{31}P are different in the two isomers. The dihedral angle calculated from the Karplus relation for POC_1H is about 34° or 110° as deduced from the 8.4 Hz for $^3J_{POCH}$.

Orientation of the Inositol Ring with Respect to the Glycerol Backbone. NOESY spectra provide a means to monitor spatial proximities of protons. For small molecules, an NOE is observable only if the spatial distance between two protons is less than 4 Å. NOESY spectra of both D- and L-inositol isomers of diC$_7$PI showed distinct differences (Figure 4). At the concentration used (3 mM), the samples are a 1:1 mix of monomers and micelles with fast exchange between both environments. The NOE's were positive, indicating that at this concentration these PI species form relatively small micelles. Similar cross-peaks were observed in a NOESY experiment with monomeric diC$_6$PI. However, since the mixture was racemic, differences between the isomers could not be measured. A key NOE was observed between the inositol C(2)H and one of the *sn*-3 glycerol protons in the D-inositol isomer (Figure 4A) but not in the L-inositol diC$_7$PI (Figure 4B). There was no NOE detected between the inositol C(1)H and *sn*-3 protons in either PI. The numbers adjacent to the cross-peaks in Figure 4A indicate peak volumes and were used to estimate the distance between the inositol C(2)H and the *sn*-3 proton. The distance between equatorial C(2)H and either of the two adjacent inositol axial protons [C(1)H or C(3)H] is ~2.4 Å and the corresponding volumes of the cross-peaks in the NOESY plot are 13.8 and 12.5, respectively. Using these distances

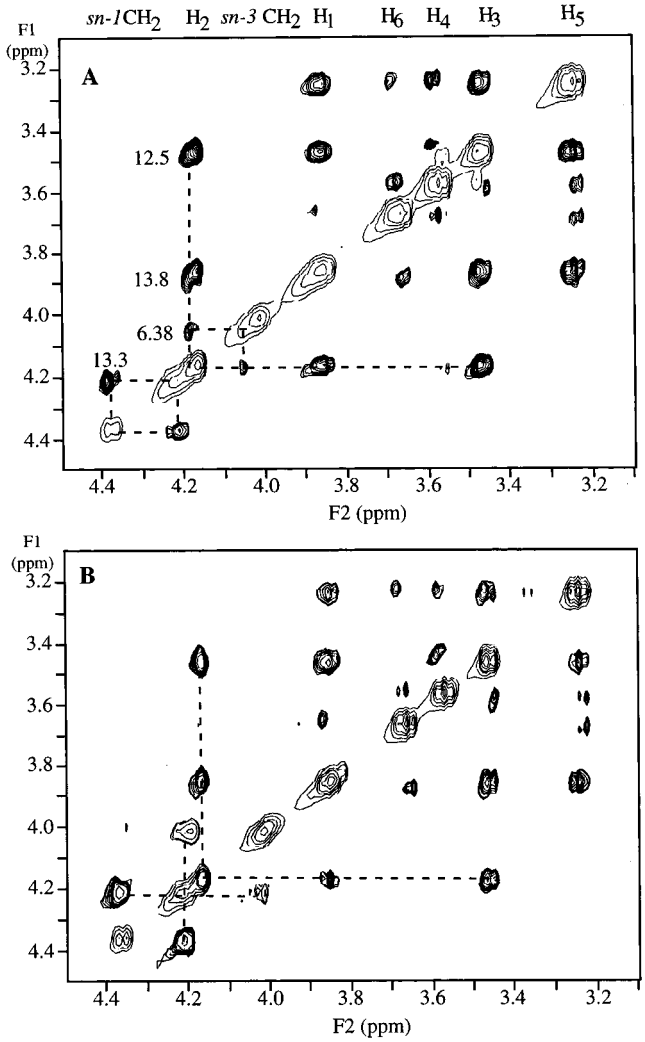

FIGURE 4: NOESY contour plots for diC$_7$PI: (A) 2.7 mM diC$_7$P-(D-)I; (B) 2.5 mM diC$_7$P(L-)I. The mixing time used was 1.0 s. The numbers in (A) represent relative cross-peak volumes. The dashed lines indicate NOEs for the inositol C_2 protons; note the cross-peak observed between H_2 and an *sn*-3 glycerol proton in the D-inositol isomer which is not present in the L-inositol isomer.

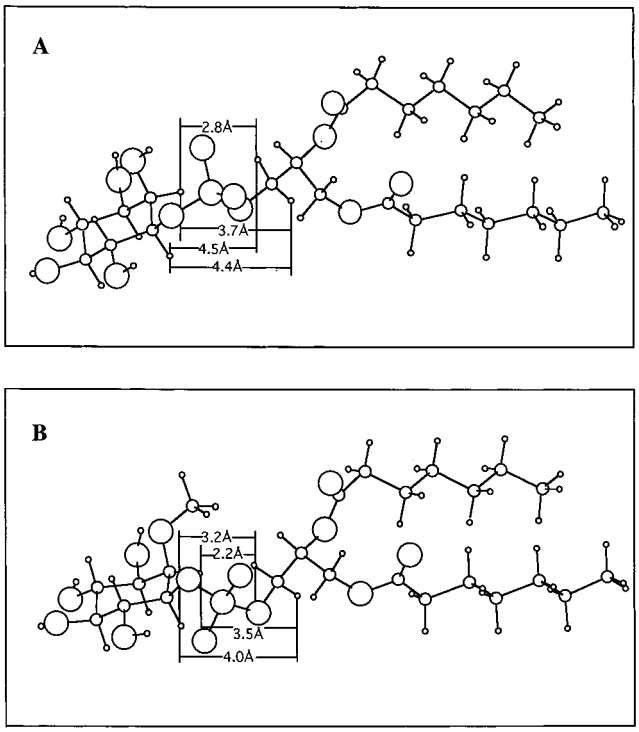

FIGURE 5: Conformation of PI and its 2-methoxy derivative obtained from computer modeling based on NOE and coupling constant constraints: (A) diC_7P(D-)I; (B) diC_7P(D-2-OCH_3)I.

as a standard, the approximate distance between C(2)H in the inositol ring and one of the *sn*-3 CH_2 protons is about 2.7 Å. This is a key constraint on the orientation of the inositol ring with respect to the glycerol backbone.

Modeling of PI Conformations. The ^{1}H NMR data were used with the QUANTA program to construct a model of diC_7P(D-)I. The positive NOE between the inositol C(2)H and glycerol *sn*-3 CH_2 and the lack of an observed NOE between C(1)H and *sn*-3 CH_2 indicate that the inositol ring must be oriented in a way that brings C(2)H near a *sn*-3 proton and C(1)H more than 4 Å from the *sn*-3 CH_2. Given the similarities in glycerol backbone coupling constants, we have modeled the glycerol backbone conformation as that in phosphatidylcholine (*10*, *28*). Packing the two chains together gives the lowest energy (CHARMm minimization), although for short-chain phospholipids significant chain segmental motion must exist. The minimized conformation for this PI molecule is shown in Figure 5A. The distances of C(2)H from the two *sn*-3 protons are 2.8 and 3.7 Å, and the distances of C(1)H from these same protons are larger than 4.4 Å. The inositol ring is nearly parallel to the chain packing direction and almost perpendicular to the membrane surface. In this model, PI adopts a fully extended conformation, leaving the phosphate center well hydrated and accessible to enzymatic attack. There are two intramolecular hydrogen bonds that would stabilize this conformation: hydroxyl groups at positions 2 and 6 in the inositol ring form hydrogen bonds with the *pro-R* and ester oxygens, respectively.

Dynamics of PI Molecules. NMR spectroscopy has the unique ability to characterize the internal motions of molecules in solution. The relaxation rates of nuclei are governed by the internal motions and overall rotational motion of the molecule. ^{13}C relaxation rates provide direct information concerning the dynamic behavior at specific sites

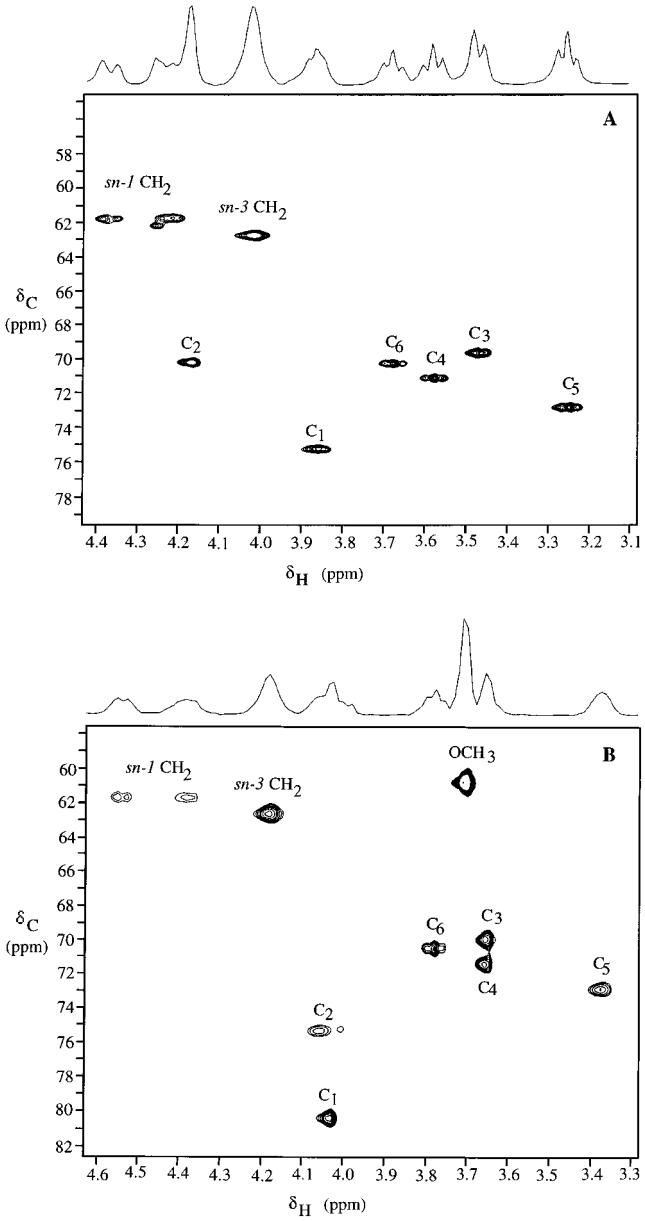

FIGURE 6: HMQC contour plots of (A) racemic diC_6PI (6 mM) and (B) diC_7P(2-OCH_3)I (0.2 mM).

in a molecule. Interpretation of protonated aliphatic carbon T_1 values can be relatively straightforward for small molecules because the longitudinal relaxation is dominated by the large ^{1}H−^{13}C dipolar interaction. The chemical shift anisotropy that contributes to the relaxation of these ^{13}C at high magnetic field strengths can be neglected (*24*). In a one-dimensional ^{13}C NMR spectrum, the carbons for CHOH at positions 2, 3, and 6 of inositol and glycerol *sn*-2 overlap. Therefore, ^{13}C spectra and chemical shifts for these molecules were assigned by HMQC. All the carbons in the inositol and glycerol region are resolved as shown in Figure 6A. The 2D pulse sequence used to measure T_1's works only for methine and not methylene carbons. There are seven such carbons in diC_6PI: six from the inositol ring and one from the glycerol backbone. T_1 values were measured for two diC_6PI concentrations: above the CMC (20 mM) and below the CMC (6 mM). The nonlinear fits of the equation $I(\tau) = I_\infty - (I_\infty - I_o)\exp(-R_1\tau)$ to the data are shown in Figure 7, and the results are listed in Table 2.

Table 2: ^{13}C T_1 Values for Racemic diC_6PI; Errors in Measurements Are Listed in Parentheses[a]

	C_1	C_2	C_3	C_4	C_5	C_6	CHO
<CMC	0.55 (0.04)	0.43 (0.02)	0.52 (0.04)	0.49 (0.02)	0.56 (0.04)	0.38 (0.04)	0.42 (0.02)
>CMC	0.50 (0.04)	0.42 (0.04)	0.50 (0.03)	0.50 (0.01)	0.47 (0.04)	0.46 (0.03)	0.36 (0.01)

[a] Concentrations of diC_6PI are 6 mM (<CMC) and 20 mM (>CMC); the CMC of this lipid in D_2O is 12.5 mM.

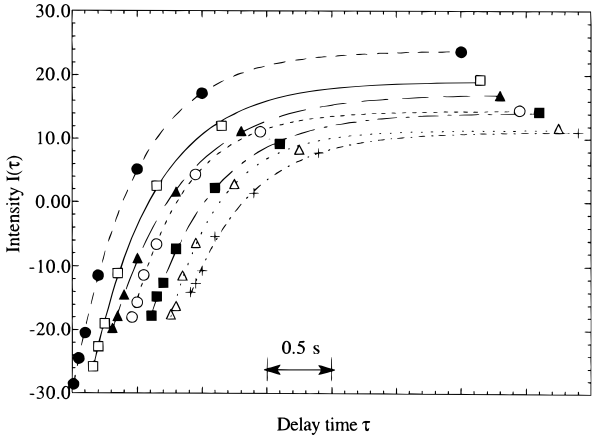

FIGURE 7: Data for ^{13}C T_1 analysis of micellar racemic diC_6PI by 2D inversion recovery measurement. Nonlinear fits of the equation $I(\tau) = I_\infty - (I_\infty - I_0)\exp(-R_1\tau)$ were applied to the data (above CMC shown): (+) C_1, (●) C_2, (□) C_3, (▲) C_4, (■) C_5, (△) C_6 of inositol ring and *sn-2* glycerol backbone (○).

Only monomers exist in solution below the CMC of diC_6-PI. T_1 values of C_1, C_3, C_4, and C_5 were around or slightly larger than 0.5 s; T_1 values for C_2 and C_6 were significantly shorter. At 20 mM PI, roughly half the molecules were aggregated in solution. Under these conditions, all T_1 values decreased except that for C_6, which increased significantly. In a micelle environment, the glycerol backbone is more constrained, and the glycerol CHO had the shortest T_1 when the molecule aggregated. T_1 values of C_1, C_3, C_4, C_5, and C_6 were almost the same, and the T_1 for C_2 was shorter, essentially the same as for monomeric PI. These T_1 values indicate that in the monomer state there are some constraints on C_2 and C_6 carbons that restrict motion. However, the constraint appears less severe for C_6 upon aggregation of diC_6PI to form micelles. This is consistent with the PI model derived from QUANTA, in which the hydroxyl groups at the 2 and 6 positions in the inositol ring form H-bonds with the *pro-R* oxygen and ester oxygen of the phosphate. Such hydrogen bonds could make both the C_2 and C_6 carbons more rigid. The observation that C_6 has a T_1 comparable to other inositol carbons when PI is packed in micelles suggests that the hydrogen bond between C(6)-OH and the phosphate ester oxygen may not exist in aggregated PI.

The ^1H T_1 values for D- and L-isomers of diC_7PI were measured by inversion recovery. These ^1H T_1 values are listed in Table 3. Basically the proton relaxation rates of the glycerol backbone and chain for two isomers are the same. The trend in ^1H T_1's in the inositol is C(4)H ≥ C(6)H > C(5)H > C(2)H > C(3)H > C(1)H for both isomers. Interestingly, the T_1 values of C(2)H and C(6)H are shorter in the D-isomer than in the L-isomer. In the D-isomer, C(2)H and C(6)H may relax through proximity to other spins or constrained motion. For example, one of the *sn*-3 glycerol protons for C(2)H is sufficiently close and motional constraints through a hydrogen bond for both the C(2)H and C(6)H to reduce ^1H T_1's for both these protons.

Table 3: ^1H T_1 Values of D- and L-Phosphatidylinositol Isomers

name		chemical shift (ppm)	T_1 (s) diC_7P(L-)I	T_1 (s) diC_7P(D-)I
backbone	*sn*-3 CH_2	4.02	0.43	0.43
	sn-1 CH_a	4.37	0.43	0.43
	sn-1 CH_b	4.22	0.43	0.43
	sn-2 CH_c	5.25	1.0	1.0
inositol headgroup	H_1	3.86	0.87	0.87
	H_2	4.17	1.2	1.0
	H_3	3.47	0.94	0.94
	H_4	3.58	1.9	1.9
	H_5	3.25	1.4	1.3
	H_6	3.67	1.9	1.6
acyl chain	CH_3	0.80	1.9	1.8
	$(CH_2)_n$	1.22	1.2	1.2
	β-H	1.54	0.79	0.72
	α-H	2.33	0.79	0.72
		2.37	0.79	0.72

Conformation of $DiC_7P(2\text{-}OCH_3)I$. Bacterial PI-PLC as well as some mammalian PI-PLC enzymes have been proposed to catalyze the hydrolysis of PI in discrete steps: (i) an intramolecular phosphotransfer reaction to form inositol cyclic 1,2-monophosphate, followed by (ii) hydrolysis of the cyclic phosphate diester to produce inositol 1-phosphate. The hydroxyl group at C(2) in the inositol ring is assumed necessary to form the cyclic product. Consistent with this mechanism, $diC_7P(2\text{-}OCH_3)I$ was a potent inhibitor of PI-PLC (*21*). However, interpretation of the inhibition results as being proof of an absolute requirement for an intramolecular phosphate transfer requires knowledge of the modified PI structure. Introduction of the bulky methyl group could substantially alter the PI conformation and packing, and this could in turn make it a nonsubstrate. For example, a nonspecific PLC from *Listeria monocytogenes* can hydrolyze PI at a rate ~1000-fold lower than a phosphatidylcholine substrate (*29*); there is no cyclic 1,2-monophosphate intermediate observed, and the final product is inositol-1-P. Based on its similarity to other nonspecific PLC enzymes, the enzyme from *L. monocytogenes* should proceed by an in-line attack of an activated water molecule on the phosphodiester bond. DiC_7PI (5 mM) is a substrate, albeit a poor one, for that enzyme. Significant hydrolysis (>20%) was detected by ^{31}P NMR assay in 6−10 h. In contrast, $diC_7P(2\text{-}OCH_3)I$ at comparable concentrations was not hydrolyzed over a period of several weeks. Does this result indicate that the nonspecific PLC from *L. monocytogenes* must first carry out an intramolecular phosphotransferase reaction?

^1H NMR analyses of the conformation of this 2-methoxy-PI were undertaken to address this question. The introduction of a methoxy group in the 2-position of inositol increased the hydrophobicity of diC_7PI, noted in a lower CMC (<0.5 mM) and enhanced micelle growth, which broadened ^1H features considerably. Only C(5)H and C(6)H exhibited well-resolved triplets. The C(2)H resonance overlapped that of C(1)H while C(3)H and C(4)H were overlapped as indicated by the HMQC spectrum (Figure 6B). The order

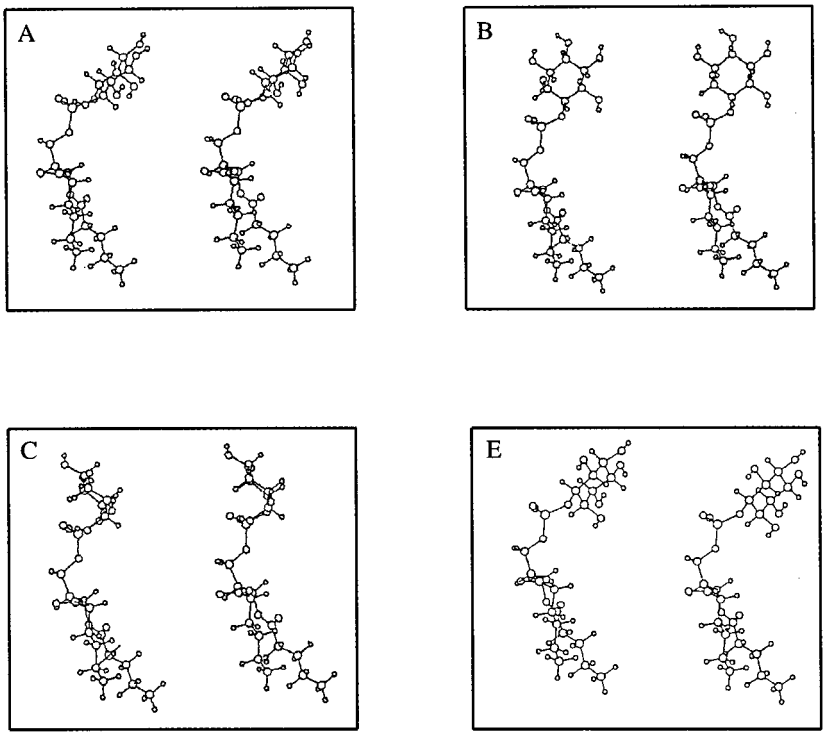

FIGURE 8: Stereoview of the four most probable conformations (A, B, C, and E) for the headgroup of membrane-bound dimyristoyl-PI. The conformation of the phosphatidyl portion is based on that of phosphatidylcholine [adapted from (*18*)].

of inositol chemical shifts in diC_7P(2-OCH_3)I is C(5)H, C(3)H ~ C(4)H, OCH_3, C(6)H, C(2)H, C(1)H, from high to low field. The ^{13}C shifts were also altered with C(1) and C(2) moving downfield about 5 ppm. The phosphate resonance was also shifted downfield slightly.

The broad line widths ($\Delta\upsilon_{1/2}$) in the ^{1}H spectrum indicated that 2-methoxy-PI forms large micelles. NOESY spectra were also consistent with this since the observed NOEs were now negative. Nonetheless, several distinct intramolecular NOEs were observed. An NOE was observed between the OCH_3 and C(2)H or C(1)H. This most likely reflects an interaction between methoxy protons and inositol C(2)H. A small NOE was observed between C(1)H or C(2)H and the *sn*-3 protons, similar to what was seen in diC_7P(D-)I. The cross-peak was too close to the diagonal peak and sensitive to line shape, phase error, etc. for accurate volume determination. Based on the diC_7P(D-)I conformation, we introduced a methyl group on the inositol C-2 oxygen and tried energy minimization. The resulting structure (Figure 5B) showed that the 2-methoxy group blocks one side of the phosphate. The distance between H_1, H_2, and the *sn*-3 protons is less than 4 Å, consistent with the NOE data. The observation that diC_7P(2-OCH_3)I is not a substrate for the nonspecific PLC is consistent with the methoxy group blocking access of the phosphodiester bond to an activated water.

DISCUSSION

The preferred orientation of the polar head groups in phosphatidylcholine and phosphatidylethanolamine is parallel to the surface. There is a relatively large change in hydration as molecules go from monomers to a micellar environment. It is reflected by changes in the ^{31}P chemical shifts which move upfield as monomers aggregate into micelles; diC_6PC shows an upfield shift of 0.18 ppm (*30*). In contrast, there is little change in δ_p as diC_6PI molecules aggregate to form micelles. This is consistent with the proposed model for PI in which the inositol moiety is perpendicular to the surface where little change in hydration occurs upon micelle formation. Short-chain PI appears to form small micelles where the molecule tumbles very fast in solution (at a rate between 10^{11} and 10^6 Hz). In a deuterium NMR study of long-chain PI (*18*), there were six conformations consistent with the experimental data (various ring quadrupolar coupling constants). The NOE data presented here rule out several of these and are consistent with the lowest potential energy conformation with intramolecular hydrogen bonds (Figure 8C). This structure was further confirmed for monomeric PI by the trends observed in ^{13}C T_1's.

However, the ^{13}C T_1 study of PI suggests that the hydrogen bond between C(6)-OH and phosphate ester oxygen may not exist in aggregated PI. The bacterial PI-PLC enzyme from *Bacillus thuringiensis* exhibits 5−6-fold "interfacial activation" when its substrate is aggregated in a micelle as opposed to existing as a monomer in solution (*21*). The mechanism for this kinetic activation is unclear. The breaking of the hydrogen bond of the hydroxyl group at position 6 and phosphate ester oxygen correlates with micelle formation and could possibly have a role in the activation, possibly by presenting the substrate in a more favorable orientation. With many other phospholipids, there is little change in conformation of the headgroup when the molecule aggregates. For PI, aggregation induces a change that could be translated to altered substrate binding by the enzyme. Furthermore, the observation that this substrate hydrogen bond is not necessary for enzyme activity could help rationalize why bacterial PI-PLC can cleave GPI anchors where the hydroxyl group at position 6 is covalently attached to glucosamine.

In the PI-PLC catalytic reaction, the first step is intramolecular and requires a hydroxyl group at position 2 of the inositol ring in order to form the cyclic product [D-*myo*-inositol 1,2-(cyclic)-phosphate]. The hydrogen bond between

the hydroxyl group at position 2 with the *pro-R* oxygen may orient the hydroxyl group for an "in-line" attack. Replacing the hydroxyl group at position 2 with a methoxy group generated a good inhibitor. This indicated that a free hydroxyl group at position 2 is not important for ligand binding to the protein in contrast to the hydroxyl group at position 3 (*31*). The computer model of diC_7P(2-OCH_3)I suggests that the methoxy group blocks one side of the phosphate, and this could explain the observation that nonspecific PLC enzymes are also unable to hydrolyze diC_7P(2-OCH_3)I. The net result is that this mechanism-based inhibitor cannot be reliably used to confirm the necessity of an inositol intramolecular phosphotransfer reaction. A better mechanism-based inhibitor of PI-PLC enzymes should replace the hydroxyl group at position 2 of the inositol ring with a smaller group such as a proton or fluorine.

REFERENCES

1. Michell, R. H. (1992) *Trends Biochem. Sci. 17*, 274−276.
2. Berridge, M. J., and Irvine, R. F. (1989) *Nature 341*, 197−205.
3. Berridge, M. J. (1987) *Annu. Rev. Biochem. 56*, 159−193.
4. Nishizuka, K. (1986) *Science 233*, 305−312.
5. Englund, P. L. (1993) *Annu. Rev. Biochem. 62*, 121−138.
6. Low, M. G., and Saltiel, A. R. (1988) *Science 239*, 268−275.
7. Ferguson, M. A. J., Homans, S. W., Dwek, R. A., and Rademacher, T. W. (1988) *Science 239*, 753−759.
8. Ikezawa, H. (1991) *Cell Biol. Int. Prep. 15*, 1115−1131.
9. Elder, M., Hitchcock, P., and Mason, R. (1977) *Proc. R. Soc. London, Ser. A 354*, 157−170.
10. Hauser, H., Pascher, I., Pearson, R. H., and Sundell S. (1981) *Biochim. Biophys. Acta 650*, 21−51.
11. Pascher, I., Sundell, S., and Hauser, H. (1981) *J. Mol. Biol. 153*, 791−806.
12. Strenk, L. M., Westerman, P. W., and Doane, J. W. (1985) *Biophys. J. 48*, 765−773.
13. Jarrell, H. C., Jorall, P. A., Giziewicz, J. B., Turner, L. A., and Smith, I. C. P. (1987) *Biochemistry 26*, 1805−1811.
14. Renou, J. P., Giziewicz, J. B., Smith, I. C. P., and Jarrell, H. C. (1989) *Biochemistry 28*, 1804−1814.
15. Ram, P., and Prestegard, J. H. (1988) *J. Am. Chem. Soc. 110*, 2383−2389.
16. Shibata, T., Uzawa, J., Sudiura, Y., Hayashi, K., and Takizawa, T. (1984) *Chem. Phys. Lipids 34*, 107−113.
17. Bushby, R. J., Byard, S. J., Hansbro, P. M., and Reid, D. G. (1990) *Biochim. Biophys. Acta 1044*, 231−236.
18. Hansbro, P. M., Byard, S. J., Bushby, R. J., Turnbull, P. J. H., Boden, N., Saunders, M. R., Novelli, R., and Reid, D. G. (1992) *Biochim. Biophys. Acta 1112*, 187−196.
19. Garigapati, V. R., and Roberts, M. F. (1993a) *Tetrahedron Lett. 34*, 769−772.
20. Garigapati, V. R., and Roberts, M. F. (1993b) *Tetrahedron Lett. 34*, 5579−5582.
21. Lewis, K. A., Garigapati, V. R., Zhou, C., and Roberts, M. F. (1993) *Biochemistry 32*, 8836−8841.
22. Zhou, C., Wu, Y., and Roberts, M. F. (1997) *Biochemistry 36*, 347−355.
23. Tan, C. A., and Roberts, M. F. (1996) *Biochim. Biophys. Acta 1298*, 58−68.
24. Palmer, A. G., Rance, M., and Wright, P. E. (1991) *J. Am. Chem. Soc. 113*, 4371−4380.
25. Nicholson, L. K., Kay, L. E., Baldisseri, D. M., Arango, J., Young, P. E., Bax, A., and Torchia, D. A. (1992) *Biochemistry 31*, 5253−5263.
26. Hauser, H., Pascher, I., and Sundell, S. (1988) *Biochemistry 27*, 9166−9174.
27. Pascher, I., Lundmark, M., Nyholm, Per-Geory, and Sundell, S. (1992) *Biochim. Biophys. Acta 1113*, 339−373.
28. Seelig, J., Gally, H., and Wohllgemuth, R. (1977) *Biochim. Biophys. Acta 467*, 109−119.
29. Goldfine, H., Johnston, N. C., and Knob, C. (1993) *J. Bacteriol. 175*, 4298−4306.
30. Pluckthun, A., and Dennis, E. A. (1981) *J. Phys. Chem. 85*, 678−683.
31. Bruzik, K. S., Hakeem, A. A., and Tsai, M.-D. (1994) *Biochemistry 33*, 8367−8374.

BI9716175